higher order diagrams and that of an isolated quasiparticle. The $\hat{\epsilon}_k$ which enters in $\hat{\xi}_k=(\Delta_k^2+\hat{\epsilon}_k^2)^{1/2}$ is closely related to the normal single-particle energy computed by Brueckner *et al.*[21] ($m^*/m\sim 0.7$), but the intermediate-state energies [which enter both in the T-matrix series and explicitly in the integral for G^b, Eq. (5.2)] are more closely related to the reference spectrum of Bethe, Brandow, and Petschek. The reference spectrum energies are characterized by a larger effective mass ($m^*\sim 0.85$) and an additive constant.

(b) It would be useful to repeat our calculations with the best phenomenological potentials (with explicit use of one-pion exchange), thus including the effects of relative angular-momentum states beyond $l=0$. In that case it would also be interesting to determine the anisotropy of the gap with respect to some arbitrary direction.

The results of our calculation lead us to believe that the energy gap in infinite nuclear matter is very small, if not absent. This suggests that the gap may well be a finite-size effect, and work is in progress to determine whether this is indeed the case.

ACKNOWLEDGMENTS

The authors are grateful to Dr. B. A. Jacobsohn, Dr. A. Bohr, Dr. B. R. Mottelson, and Dr. D. Falk for illuminating discussions and comments. They wish to thank J. Hartle, R. Kennedy, and W. Shaw for valuable assistance in various phases of the numerical computations.

PHYSICAL REVIEW VOLUME 133, NUMBER 5B 9 MARCH 1964

Energy Gap in Nuclear Matter. II. BCS Theory*

R. KENNEDY, L. WILETS, AND E. M. HENLEY
University of Washington, Seattle, Washington

(Received 10 October 1963)

The Bardeen-Cooper-Schrieffer (BCS) theory is employed to study the energy gap in nuclear matter with various internucleonic potentials which fit singlet low-energy scattering data and the s-wave phase shift at 310 MeV. The interactions are expressed as the sum of two terms, each of which is separable, thus admitting exact solutions of the energy-gap equation. The dependence of the energy gap on the form and parameters of the interaction, as well as on the nuclear density and effective mass, is investigated. For normal nuclear density, the gap is found to be small compared with that observed in the heaviest nuclei.

I. INTRODUCTION

THE prediction of an energy gap in the spectrum of a superconductor by the theory of Bardeen, Cooper, and Schrieffer[1] (BCS) and observations on the spectra of even-even nuclei have led to the speculation that the same concepts might apply to nuclei[2] and nuclear matter.[3,4] An essential feature of a superconducting system is the attractive interaction of time-reversed pairs near the Fermi surface. The present paper uses this feature to study the energy gap in infinite nuclear matter.

Solutions of the basic integral equation are obtained which qualitatively confirm the results of Emery and Sessler,[5] who used a Gammel-Thaler potential acting in s waves only. In addition, we show the effects on the gap of different forms of the potential between nucleons, define criteria for the existence of an energy gap (see also Ref. 4), and compare approximate solutions with exact solutions of the integral equations.

II. ENERGY GAP FOR A SINGLE SEPARABLE INTERACTION

The basic equation to be solved is the BCS integral equation[1] (for notation, see Ref. 6; however, we use here Δ_k for the quantity Δ_k^0)

$$\Delta_k=-\tfrac{1}{2}\sum_{k'}\frac{\Delta_{k'}G_{k,k'}^0}{(\hat{\epsilon}_{k'}^2+\Delta_{k'}^2)^{1/2}}.$$

The energy gap is interpreted as $2\Delta_{k_F}\equiv 2\Delta$. $\hat{\epsilon}_{k'}$ is a renormalized single-particle energy measured with respect to the Fermi energy and $G_{k,k'}^0$ is the free-particle-interaction matrix element

$$G_{k,k'}^0=\langle \mathbf{k}, -\mathbf{k}|V|\mathbf{k}', -\mathbf{k}'\rangle.$$

Throughout this paper only the s-wave part of this matrix is used, and $\hat{\epsilon}_k$ is represented by the effective-

* Supported in part by the U. S. Atomic Energy Commission under Contract A.T.(45-1)1388, Program B.

[1] J. Bardeen, L. N. Cooper, and J. R. Schrieffer, Phys. Rev. **108**, 1175 (1957).

[2] A. Bohr, B. R. Mottelson, and D. Pines, Phys. Rev. **110**, 936 (1958).

[3] L. N. Cooper, R. L. Mills, and A. M. Sessler, Phys. Rev. **114**, 1377 (1959).

[4] R. L. Mills, A. M. Sessler, S. A. Moszkowski, and D. G. Shankland, Phys. Rev. Letters **3**, 381 (1959).

[5] V. J. Emery and A. M. Sessler, Phys. Rev. **119**, 248 (1960).

[6] E. M. Henley and L. Wilets, preceding paper, Phys. Rev. **133**, B1118 (1964).

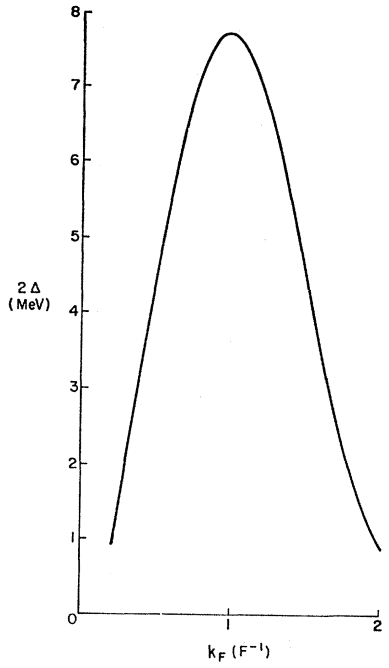

FIG. 1. Energy gap for the simple Yamaguchi potential. $m^*/m=1$.

mass approximation

$$\hat{\epsilon}_k=(\hbar^2/2m^*)(k^2-k_F^2).$$

The usual transition to the continuum is made by $\Sigma\rightarrow 1/(2\pi)^3\int d^3\mathbf{k}$, unit volume normalization, $G_{k,k'}{}^0\rightarrow G^0(k,k')$ (s wave only) which gives

$$\Delta(k)=\frac{-2\pi}{(2\pi)^3}\int_0^\infty\frac{\Delta(k')G^0(k,k')k'^2dk'}{[\hat{\epsilon}^2(k')+\Delta^2(k')]^{1/2}}. \tag{1}$$

The difficulty in solving Eq. (1) is posed in large part by the nonlinear occurrence of $\Delta(k')$. However, if $G^0(k,k')$ is a finite sum of separable terms

$$G^0(k,k')=(\hbar^2/m)(2\pi)^3\Sigma_\alpha\lambda_\alpha w_\alpha(k)w_\alpha(k'),$$

(the factor $\hbar^2/m$ is introduced for convenience), then the solution reduces to a system of nonlinear transcendental equations. (This is analogous to the situation with a linear integral equation where the reduction is to a system of linear algebraic equations.) A simple example of such a separable potential is furnished by the Yamaguchi[7] potential:

$$G^0(k,k')=-\frac{\lambda\hbar^2}{m}(2\pi)^3\frac{1}{(k^2+\beta^2)(k'^2+\beta^2)}$$
$$\equiv-\frac{\lambda\hbar^2}{m}(2\pi)^3w(k)w(k').$$

The BCS equation becomes

$$\Delta(k)=\frac{2\pi\hbar^2}{m}\lambda w(k)\int_0^\infty\frac{\Delta(k')w(k')k'^2dk'}{[\hat{\epsilon}^2+\Delta^2(k')]^{1/2}},$$

which is satisfied by $\Delta(k)=Aw(k)$. The constant A is determined by solving the equation

$$1=\frac{2\pi\hbar^2}{m}\lambda\int_0^\infty\frac{k'^2w^2(k')dk'}{[\hat{\epsilon}^2+A^2w^2(k')]^{1/2}}. \tag{2}$$

Figure 1 shows the solution of Eq. (2) as a function of the Fermi momentum for the potential parameters given at the end of Table I.

Although Eq. (2) can be solved numerically to any desired degree of accuracy, a good approximation for small Δ is as follows:

$$1\approx\frac{2\pi\hbar^2}{m}\lambda\Bigg[\int_0^{k_F-k_c}\frac{k'^2w^2(k')dk'}{|\hat{\epsilon}|}+\int_{k_F+k_c}^\infty\frac{k'^2w^2(k')dk'}{|\hat{\epsilon}|}$$
$$+k_F^2w^2(k_F)\int_{k_F-k_c}^{k_F+k_c}\frac{dk'}{\{[(\hbar^2/m^*)k_F(k-k_F)]^2+\Delta^2\}^{1/2}}\Bigg], \tag{3a}$$

which is valid when

$$\frac{m^*\Delta}{\hbar^2k_F}\ll k_c\ll\beta,k_F. \tag{3b}$$

Further, the last integral in (3a) is, to the same approximation,

$$\frac{2m^*w^2(k_F)k_F}{\hbar^2}\ln\frac{2\hbar^2k_Fk_c}{m^*\Delta}.$$

Let

$$I(\beta)=\frac{2\pi\hbar^2\lambda}{m}\Bigg[\int_0^{k_F-k_c}\frac{k'^2w^2(k')dk'}{|\hat{\epsilon}|}+\int_{k_F+k_c}^\infty\frac{k'^2w^2(k')dk'}{|\hat{\epsilon}|}\Bigg],$$

then

$$\Delta=\frac{2\hbar^2k_Fk_c}{m^*}\exp\Bigg[-\frac{m}{4\pi m^*k_Fw^2(k_F)\lambda}(1-I(\beta))\Bigg]. \tag{4}$$

$I(\beta)$ is evaluated in Appendix A. The cutoff k_c is chosen so that the solutions to the exact expression match on smoothly to those of the approximation, subject to the restriction (3b) above.

Finally, it is interesting to note that a finite energy gap always exists for λ positive because the potential is then everywhere attractive.

III. THE NUCLEAR ENERGY GAP

A. Specification of Potentials

To investigate the energy gap in nuclear matter, it is necessary to consider more "realistic" potentials which are able to reproduce relevant nucleon-nucleon scattering data. Since the most important short-range effects occur for relative singlet s states, we consider effective interactions for this state only. Because the form of the interaction is not completely determined by the scattering phase shifts at a finite number of points, it is of interest to examine the effect of the shape on the energy gap. For this reason two families of potentials—two

[7] Y. Yamaguchi, Phys. Rev. **95**, 1628 (1954).

distinct members of each—are compared. Three of these fit the same three parameters deduced from singlet scattering data: the scattering length, effective range, and the s-wave phase shift at 310 MeV. The fourth potential is the one suggested by Puff.[8] The point at 310 MeV is chosen because the phase shifts are best known there from the work of Stapp, Ypsilantis, and Metropolis[9] together with the work of MacGregor, Moravcsik, and Stapp.[10]

The forces we discuss here are all sums of two separable terms and they fall into two classes. In the first class both terms have the simple Yamaguchi form (s wave only):

$$V(r,r')=\frac{\pi\hbar^2}{2m}\left[\lambda_1\frac{e^{-\beta_1 r}}{r}\frac{e^{-\beta_1 r'}}{r'}-\lambda_2\frac{e^{-\beta_2 r}}{r}\frac{e^{-\beta_2 r'}}{r'}\right].$$

These will be referred to as "back-to-back" Yamaguchi's. The second class of potentials (called Puff type) obtain their repulsion from a hard shell and their attraction from a simple Yamaguchi form

$$V(r,r')=\frac{\pi\hbar^2}{2m}\lim_{\lambda_c\to\infty}\left[\lambda_c\frac{\delta(r-r_c)}{r}\frac{\delta(r'-r_c)}{r'}-\lambda\frac{e^{-\beta r}}{r}\frac{e^{-\beta r'}}{r'}\right],$$

where r_c is the shell radius. Their Fourier transforms,

$$G^0(\mathbf{k},\mathbf{k}')=\int e^{-\mathbf{k}\cdot\mathbf{r}}V(r,r')e^{-\mathbf{k}'\cdot\mathbf{r}'}d^3r d^3r',$$

are, respectively,

$$\frac{\hbar^2}{m}(2\pi)^3\left[\frac{\lambda_1}{(k^2+\beta_1^2)(k'^2+\beta_1^2)}-\frac{\lambda_2}{(k^2+\beta_2^2)(k'^2+\beta_2^2)}\right],$$

and

$$\frac{\hbar^2}{m}(2\pi)^3\lim_{\lambda_c\to\infty}\left[\lambda_c\frac{\sin kr_c}{k}\frac{\sin k'r_c}{k'}-\frac{\lambda}{(k^2+\beta^2)(k'^2+\beta^2)}\right].$$

The three scattering parameters described earlier completely determine the constants of the Puff-type

TABLE I. Potential parameters.

	I. Back-to-back Yamaguchi			
	$\beta_1(\mathrm{F}^{-1})$	$\lambda_1(\mathrm{F}^{-3})$	$\beta_2(\mathrm{F}^{-1})$	$\lambda_2(\mathrm{F}^{-3})$
a	3.	7.65507	1.76599	1.73131
b	6.	123.075	1.62047	0.952992
	II. Puff type			
		$\beta(\mathrm{F}^{-1})$	$\lambda(\mathrm{F}^{-3})$	$r_c(\mathrm{F})$
c (Puff-type II)		1.60152	0.886015	0.256986
d (Puff-type I)		2.004	3.64	0.45
	III. Simple Yamaguchi			
	$\beta(\mathrm{F}^{-1})$		$\lambda(\mathrm{F}^{-3})$	
	1.254		0.18725	

[8] R. D. Puff, Ann. Phys. (N. Y.) **13**, 319 (1961).
[9] H. P. Stapp, T. J. Ypsilantis, and N. Metropolis, Phys. Rev. **105**, 302 (1957).
[10] M. H. MacGregor, M. J. Moravcsik, and H. P. Stapp, Ann. Rev. Nucl. Sci. **10**, 291 (1960).

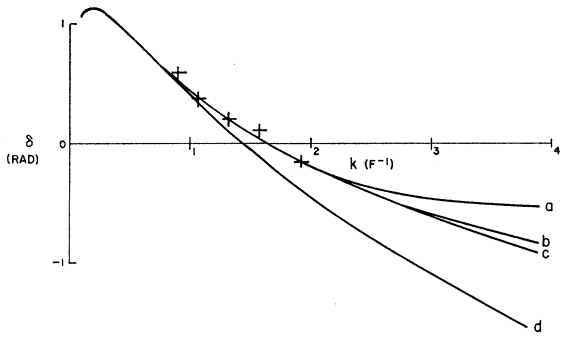

FIG. 2. Phase shifts for the sets of potential parameters given in Table I. The +'s represent the best experimental points (see Ref. 8). Curves a, b, and c all pass through the experimental point at $k=1.933$ F^{-1} which corresponds to 310 MeV.

interaction. Since the back-to-back Yamaguchi's have four arbitrary constants, they form an infinite family that can fit the chosen scattering data. We shall compare two particular choices from this family with the Puff potential[8] and Puff-type interaction. The constants used are specified in Table I, and their determination is given in Appendix B. In Fig. 2, the values of the phase shift have been plotted as a function of the relative momentum for all the potentials in Table I except the simple Yamaguchi. The experimental points are the best set specified by Stapp *et al.*[10] The Puff[8] potential (curve d of Fig. 2) gives a greater negative phase shift at 310 MeV than do the others. However, it contains a currently acceptable value of the hard-shell radius and so is included.

B. Solutions of the Gap Equation

The form of all the phenomenological nucleon-nucleon potentials of Sec. III is

$$G^0(k,k')=\frac{\hbar^2}{m}(2\pi)^3[\lambda_1 w_1(k)w_1(k')-\lambda_2 w_2(k)w_2(k')], \quad (5)$$

which allows the following solution of the integral equation (1):

$$\Delta(k)=Aw_1(k)+Bw_2(k), \quad (6)$$

where A and B are independent of k,

$$A=-\frac{2\pi\hbar^2}{m}\lambda_1\int_0^\infty\frac{k'^2\Delta(k')w_1(k')dk'}{[\hat{\epsilon}^2(k')+\Delta^2(k')]^{1/2}}, \quad (7)$$

and

$$B=\frac{2\pi\hbar^2}{m}\lambda_2\int_0^\infty\frac{k'^2\Delta(k')w_2(k')dk'}{[\hat{\epsilon}^2(k')+\Delta^2(k')]^{1/2}}. \quad (8)$$

When $\Delta(k)$ from expression (6) is substituted in Eqs. (7) and (8), the following two equations are obtained:

$$\lambda_1(AI_1+BI_2)-A=0, \quad (9a)$$

and

$$\lambda_2(BI_3-AI_2)-B=0, \quad (9b)$$

where the integrals I_1, I_2, and I_3 are functions of both A and B:

$$\begin{bmatrix} I_1 \\ I_2 \\ I_3 \end{bmatrix} = \frac{2\pi\hbar^2}{m} \int_0^\infty \frac{k^2 dk}{[\hat{\epsilon}^2 + (Aw_1(k) + Bw_2(k))^2]^{1/2}} \begin{bmatrix} -w_1^2(k) \\ -w_1(k)w_2(k) \\ w_2^2(k) \end{bmatrix}.$$

For the Puff-type potential $\lambda_1 \to \infty$, and Eqs. (9) reduce to

$$AI_1 + BI_2 = 0,$$

and

$$I_1 = \lambda_2(I_2^2 + I_1 I_3).$$

For each interaction, these sets of exact nonlinear equations were solved numerically by an iterative scheme on an IBM-709 digital computer. For small Δ, the approximation made in Sec. II can be employed. The answers can be expressed as follows:

$$\Delta = \frac{2\hbar^2 k_F k_c}{m^*} e^{-(m/4\pi m^*)(Y/X)}. \tag{10}$$

For the Puff-type potentials, Y and X are given by

$$Y = I_4(I(\beta) - 1) - I_5^2,$$
$$X = k_F\lambda_2[2I_5 w_1(k_F)w_2(k_F) - I(\beta)w_1^2(k_F) - I_4 w_2^2(k_F) + w_1^2(k_F)],$$

with

$$I_4 = \frac{2\pi\hbar^2}{m}\lambda_2\left(\int_0^{k_F - k_c} + \int_{k_F + k_c}^\infty\right)\frac{k^2 w_1^2(k)dk}{|\hat{\epsilon}|},$$

$$I_5 = \frac{2\pi\hbar^2}{m}\lambda_2\left(\int_0^{k_F - k_c} + \int_{k_F + k_c}^\infty\right)\frac{k^2 w_1(k)w_2(k)dk}{|\hat{\epsilon}|},$$

where $w_1(k) = k^{-1}\sin k r_c$, $w_2(k) = (k^2 + \beta^2)^{-1}$, and $m^*\Delta/\hbar^2 k_F \ll k_c \ll \beta$, k_F, r_c^{-1}. Explicit formulas for I_4 and I_5 are given in Appendix A. For the back-to-back Yamaguchi potentials, Y and X are given by

$$Y = I(\beta_1)I(\beta_2) - I_6^2 + I(\beta_2) - I(\beta_1) - 1,$$
$$X = k_F[2I_6 w_1(k_F)w_2(k_F)(\lambda_1\lambda_2)^{1/2} - \lambda_1 I(\beta_2)w_1^2(k_F) - \lambda_2 I(\beta_1)w_2^2(k_F) + \lambda_1 w_1^2(k_F) - \lambda_2 w_2^2(k_F)],$$

with

$$I_6 = \frac{2\pi\hbar^2}{m}(\lambda_1\lambda_2)^{1/2}\left(\int_0^{k_F - k_c} + \int_{k_F + k_c}^\infty\right)\frac{k^2 w_1(k)w_2(k)dk}{|\hat{\epsilon}|},$$

where $w_1(k) = (k^2 + \beta_1^2)^{-1}$, $w_2(k) = (k^2 + \beta_2^2)^{-1}$, and $m^*\Delta/\hbar^2 k_F \ll k_c \ll \beta_1$, β_2, k_F. The explicit formula for I_6 is given in Appendix A.

From the small Δ approximation [Eq. (10)], it can be seen that the exact condition for the limit of a vanishing energy gap is $X = 0$. This is to be contrasted with the purely attractive case where a nonzero solution always exists (if $\lambda > 0$). The condition $X = 0$ thus furnishes a criterion for the existence of the energy gap in terms of the parameters of the problem.

IV. RESULTS AND CONCLUSIONS

Figure 3 shows the energy gap as a function of the Fermi momentum [$\sim$(density)$^{1/3}$] for all of the

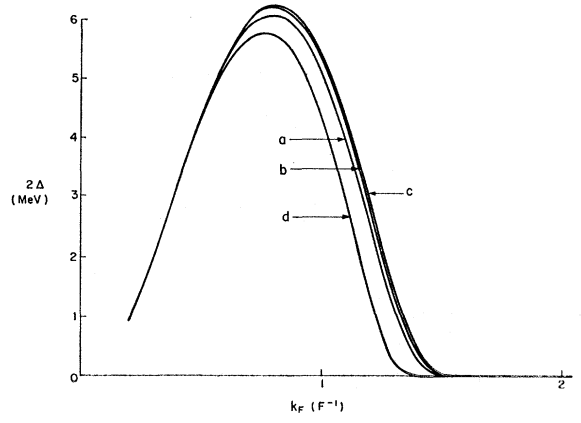

FIG. 3. Energy-gap curves for the potentials given in Table I. $m^*/m = 1$.

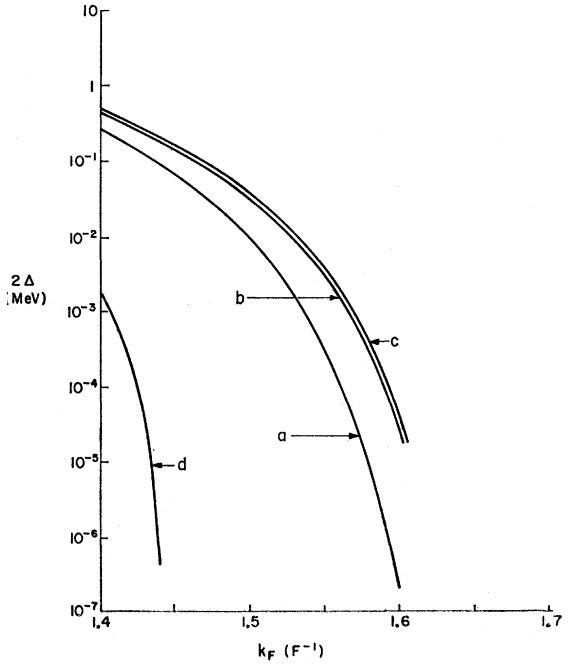

FIG. 4. An extension of the curves given in Fig. 3. $m^*/m = 1$.

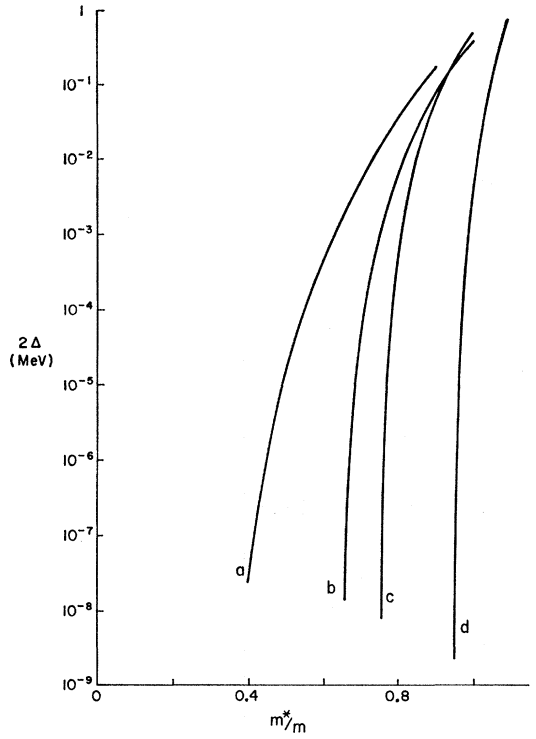

FIG. 5. Energy-gap curves for $k_F=1.4$ F^{-1}.

potentials investigated. Note that although three of the potentials (*a*, *b*, and *c*) fit the same three pieces of scattering data, the curves are not identical. This is partially caused by the fact that the interactions differ at and close to the Fermi surface, where the chief contribution to the integrals arises. However, in the region of low nuclear density (i.e., $k_F \lesssim 1.3$ F^{-1}), the dependence on the form and parameters of the potential is not great.

Figure 4 is a continuation of Fig. 3 for higher nuclear densities to the region where the gap is extremely small. Because of the nonanalytic exponential dependence of the gap parameters on k_F, slight changes in the interaction are here greatly magnified in the numerical value of Δ.

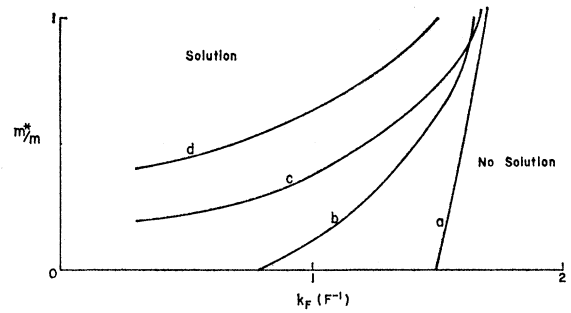

FIG. 6. Curves showing where solutions cease to exist for the potentials given in Table I.

The dependence of the energy gap on the effective mass m^* is shown in Fig. 5 at "normal" nuclear density ($r_0=1.09$ F, where the nuclear radius is $r_0 A^{1/3}$), corresponding to $k_F=1.4$ F^{-1}. Because the gap is quite small, there is a strong dependence on the potential parameters. For the suggested values of[11] $m^*/m\approx 0.7$, the gap is equal to, or less than, 5 keV.

Figure 6 shows the line of demarcation between the regions for which solutions do and do not exist. In general, the Puff-type potentials, being more repulsive at higher momenta, give a zero gap for lower Fermi momenta than do the corresponding back-to-back Yamaguchi's.

We can summarize our findings as follows: (1) The gap at normal nuclear densities and $m^*\approx 0.7m$ is very small. For the most optimistic of these potentials it is about 5 keV. This is to be compared with ~1 MeV, observed in the heaviest nuclei. (2) Our results agree roughly with those obtained by Emery and Sessler.[5] (3) The gap is extremely sensitive to small changes in the form and parameters of the interaction and to the effective mass in the range of very small gaps ($\Delta \lesssim 1$ keV) but less so when the gap is sizeable ($\Delta \gtrsim 0.1$ MeV).

APPENDIX A: EVALUATION OF INTEGRALS

In Sec. II, the integral $I(\beta)$ was introduced. Its form is

$$I(\beta)=\frac{4\pi m^*}{m}\lambda w(k_F)\left[\frac{k_F w(k_F)}{2}\ln\frac{4k_F^2-k_c^2}{k_c^2}-\frac{1}{2}\frac{k_F-k_c}{(k_F-k_c)^2+\beta^2}-\frac{1}{2}\frac{k_F+k_c}{(k_F+k_c)^2+\beta^2}\right.$$
$$\left.+\frac{1}{2\beta}(\tfrac{1}{2}-k_F^2 w(k_F))\left(\pi-2\tan^{-1}\frac{2k_F\beta}{\beta^2-k_F^2+k_c^2}\right)\right],$$

where $w(k)=(k^2+\beta^2)^{-1}$. For the hard-shell potential, the integrals (Sec. III) are defined as follows:

$$I_4=\frac{m^*\lambda}{mk_F}\left[\ln\frac{4k_F^2-k_c^2}{k_c^2}+\cos 2r_c k_F\{2\,\mathrm{Ci}[2r_c k_c]-\mathrm{Ci}[2r_c(2k_F-k_c)]-\mathrm{Ci}[2r_c(2k_F+k_c)]\}\right.$$
$$\left.+\sin 2r_c k_F\{\pi-\mathrm{Si}[2r_c(2k_F-k_c)]-\mathrm{Si}[2r_c(2k_F+k_c)]\}\right]$$

[11] K. A. Brueckner, J. L. Gammel, and J. T. Kubis, Phys. Rev. **118**, 1438 (1960).

$$I_5=2\pi\frac{m^*w_2(k_F)\lambda}{m}\{2I_{\beta r_c}[r_c(k_F-k_c)]+2I_{\beta r_c}[r_c(k_F+k_c)]+\sin r_c k_F\{\mathrm{Ci}[r_c(2k_F+k_c)]+\mathrm{Ci}[r_c(2k_F-k_c)]$$
$$-2\,\mathrm{Ci}[r_c k_c]\}+\cos r_c k_F\{\pi-\mathrm{Si}[r_c(2k_F-k_c)]-\mathrm{Si}[r_c(2k_F+k_c)]\}-\pi e^{-\beta r_c}\}.$$

$\mathrm{Si}(x)$ and $\mathrm{Ci}(x)$ are, respectively, the sine and cosine integrals, and

$$I_{\beta r_c}(x)=\int_0^x \frac{t\sin t\,dt}{t^2+(\beta r_c)^2}$$

is evaluated numerically.

$$I_6=\frac{4\pi m^*(\lambda_1\lambda_2)^{1/2}}{m(\beta_1^2-\beta_2^2)}\left[\frac{\pi}{2}(w_2(k_F)\beta_2-w_1(k_F)\beta_1)+w_1(k_F)\beta_1\tan^{-1}\frac{2k_F\beta_1}{\beta_1^2-k_F^2+k_c^2}-w_2(k_F)\beta_2\tan^{-1}\frac{2k_F\beta_2}{\beta_2^2-k_F^2+k_c^2}\right.$$
$$\left.-\frac{w_2(k_F)\beta_2^2-w_1(k_F)\beta_1^2}{2k_F}\ln\frac{4k_F^2-k_c^2}{k_c^2}\right].$$

APPENDIX B: DETERMINATION OF POTENTIAL PARAMETERS

The potential parameters given in Table I were fit to the scattering data by means of the scattering matrix (s wave only)

$$S(k,k';\Omega)=G^0(k,k')+\frac{m}{\hbar^2}\int\frac{G^0(k,k'')S(k'',k';\Omega)d^3k''}{\Omega-k''^2}.$$

In terms of S, the scattering amplitude is

$$f(k)=\lim_{\epsilon\to 0}-\frac{2\pi^2 m}{\hbar^2}S(k,k;k^2+i\epsilon)=\frac{e^{i\delta}\sin\delta}{k},$$

and we obtain

$$k\cot\delta=ik+\frac{1}{f}=ik-\frac{\hbar^2}{2\pi^2 mS(k,k;k^2+i\epsilon)}.$$

For low energies

$$k\cot\delta\approx(1/a)+\tfrac{1}{2}r_e k^2,$$

where a and r_e are the scattering length and effective range, respectively.

The form of $G^0(k,k')$ is given by Eq. (5). Then

$$S(k,k;k^2+i\epsilon)=(\hbar^2/m)[\lambda_1 w_1^2(k)-\lambda_2 w_2^2(k)+\lambda_1 w_1(k)g(k)-\lambda_2 w_2(k)h(k)],$$

where

$$h(k)=\frac{\lambda_2 w_2(k)I_{22}(\lambda_1 I_{11}-1)+\lambda_1 I_{12}(w_1(k)-\lambda_2 w_2(k)I_{12})}{\lambda_1\lambda_2 I_{12}^2-(\lambda_2 I_{22}+1)(\lambda_1 I_{11}-1)},$$

and

$$g(k)=\frac{\lambda_1 w_1(k)I_{11}(\lambda_2 I_{22}+1)-\lambda_2 I_{12}(w_2(k)+\lambda_1 w_1(k)I_{12})}{\lambda_1\lambda_2 I_{12}^2-(\lambda_2 I_{22}+1)(\lambda_1 I_{11}-1)}.$$

The integrals I_{ij} are given by

$$I_{ij}=-2\pi\int_{-\infty}^{\infty}\frac{w_i(k')w_j(k')k'^2dk'}{k'^2-k^2-i\epsilon}.$$

For the specific interactions chosen, the results are as follows: With Puff-type potentials

$$k\cot\delta=\frac{1}{w_1(k)}\left[\frac{e^{-2\beta r_c}}{2e^{-\beta r_c}-\cos kr_c-[w_1(k)/2][(1/\pi^2\lambda_2 w_2^2(k))-\beta+k^2/\beta]}-\cos kr_c\right],$$

$$\frac{1+(r_c/3a)-(r_e/r_c)}{1+(r_c/a)^2}=\left(1-\frac{3}{\beta r_c}\right)e^{2\beta r_c}+\left(\frac{1}{3}-\frac{4}{\beta^2 r_c^2}\right)\left[\frac{1}{1+(a/r_c)}-(1-e^{\beta r_c})^2\right],$$

and

$$\frac{\beta^3}{\pi^2\lambda_2}=1+\frac{2}{\beta r_c}\left[2e^{-\beta r_c}-1-\frac{e^{-2\beta r_c}}{1+r_c/a}\right],$$

where the limit $\lambda_1\to\infty$ has been taken, $w_1(k)=k^{-1}\sin kr_c$ and $w_2(k)=(k^2+\beta^2)^{-1}$. The back-to-back Yamaguchi potentials give

$$k\cot\delta=\tfrac{1}{2}[\beta_1\beta_2(\beta_1+\beta_2)^2\{(\lambda_2/\beta_2)w_2^2(k)(k^2-\beta_2^2)-(\lambda_1/\beta_1)w_1^2(k)(k^2-\beta_1^2)+(1/\pi^2)\}$$
$$-\pi^2\lambda_1\lambda_2w_1^2(k)w_2^2(k)(\beta_1-\beta_2)^2\{(k^2-\beta_1^2)(k^2-\beta_2^2)-4k^2\beta_1\beta_2\}]$$
$$\times[\beta_1\beta_2(\beta_1+\beta_2)^2(\lambda_2w_2^2(k)-\lambda_1w_1^2(k))-(\beta_1+\beta_2)\lambda_1\lambda_2\pi^2w_1^2(k)w_2^2(k)(\beta_1-\beta_2)^2(k^2-\beta_1\beta_2)]^{-1},$$

$$-\frac{2\pi^2}{a}=\frac{\beta_1\beta_2}{\beta_1+\beta_2}\frac{\beta_1^3\beta_2^3(\beta_1+\beta_2)^2-\pi^2(\beta_1+\beta_2)^2(\lambda_2\beta_1^3-\lambda_1\beta_2^3)-\lambda_1\lambda_2\pi^4(\beta_1-\beta_2)^2}{(\beta_1+\beta_2)(\lambda_1\beta_2^4-\lambda_2\beta_1^4)-\lambda_1\lambda_2\pi^2(\beta_1-\beta_2)^2},$$

and

$$-r_e\beta_1^2\beta_2^2(\beta_1+\beta_2)[(\beta_1+\beta_2)(\lambda_1\beta_2^4-\lambda_2\beta_1^4)-\lambda_1\lambda_2\pi^2(\beta_1-\beta_2)^2]$$
$$=\beta_1\beta_2[\pi^2\lambda_1\lambda_2(\beta_1-\beta_2)^2\{2(\beta_1+\beta_2)^2+\beta_1^2+\beta_2^2\}+3(\beta_1+\beta_2)^2(\lambda_2\beta_1^5-\lambda_1\beta_2^5)]$$
$$+\frac{2(\beta_1+\beta_2)}{a}[\pi^2\lambda_1\lambda_2\{(\beta_1+\beta_2)(\beta_1^3+\beta_2^3)-4\beta_1^2\beta_2^2+(\beta_1-\beta_2)^4\}+2(\beta_1+\beta_2)(\lambda_2\beta_1^6-\lambda_1\beta_2^6)],$$

where $w_1(k)=(k^2+\beta_1^2)^{-1}$, and $w_2(k)=(k^2+\beta_2^2)^{-1}$.

The scattering data used to get potentials *a*, *b*, and *c* in Table I are: $a=23.69$ F, $r_e=2.5$ F, and $\delta(310\text{ MeV})=-8.92°$. Potential *d* gives a phase shift of $-22.4°$ at 310 MeV. The simple Yamaguchi is fit to the scattering length and effective range only.